Improving Image-Based Characterization of Porous Media with Deep Generative Models

Timothy I. Anderson [* 1] **Kelly M. Guan** [* 2] **Bolivia Vega** [2] **Laura Frouté** [2] **Anthony R. Kovscek** [2]

Abstract

Micro- and nanoscale imaging are important for characterizing subsurface formations for carbon sequestration, shale gas recovery, and hydrogen storage. Common imaging techniques, however, are often sample-destructive, expensive, require high levels of expertise, or only acquire planar data. The resulting image datasets therefore may not allow for a representative estimation of rock properties. In this work, we address these challenges in image-based characterization of porous media using deep generative models. We present a machine learning workflow for characterizing porous media from limited imaging data. We develop methods for 3D image volume translation and synthesis from 2D training data, apply this method to grayscale and multimodal image datasets of sandstones and shales, and simulate flow through the generated volumes. Results show that the proposed image reconstruction and generation approaches produce realistic pore-scale 3D representations of rock samples using only 2D training data. The models proposed here expand our capabilities for characterization of rock samples and enable new understanding of pore-scale storage and recovery processes.

1. Introduction

The transition to a sustainable energy future requires a combination of greenhouse gas sequestration, long-term adoption of renewable sources of energy, and near-term fuel switching to cleaner available energy resources (EIA/ARI, 2013). Three such approaches that could contribute to each of these goals are, respectively, CO_2 sequestration, subsurface H_2 storage, and natural gas recovery (Zoback & Kohli, 2019; Hassanpouryouzband et al., 2021). One important requirement for scalable and sustainable implementation of these technologies is characterization of porous media transport properties in order to identify viable candidate reservoirs.

Image-based characterization in conjunction with digital rock physics techniques is a versatile approach for understanding properties of reservoir rocks at the pore and rock fabric scales (Ketcham & Carlson, 2001; Vega et al., 2013), but these methods often require a large number of high-contrast images. Micro- and nanoscale image datasets often suffer from data scarcity or destroy the sample during image acquisition, resulting in datasets that are either too small to estimate rock properties or preclude further experimentation. Furthermore, many relevant imaging modalities, such as electron microscopy, only acquire images in 2D, but 3D information is needed to characterize fully a rock sample.

Here we outline approaches to overcoming these limitations of reservoir rock imaging using deep generative models. We present a deep learning-based image characterization workflow, shown in Fig. 1, and outline two applications of this workflow: image modality translation for predicting image volumes when only 2D training data is available, and image synthesis for grayscale and multimodal porous media image volumes from 2D images. In what follows, we describe the imaging workflow and outline the deep learning models used for data translation and synthesis for reservoir rock images.

2. Image Modality Translation

2.1. Multimodal Imaging Overview

Multimodal imaging is an emerging method for geomaterial characterization where image data is acquired at the same scale from two or more image modalities (Aljamaan et al., 2017). While multimodal imaging is commonplace in medical imaging (Torrado-Carvajal et al., 2016; Cao et al., 2018), substantially less prior work has applied multimodal imaging to the characterization of subsurface samples.

Micro- and nanoimaging modalities often present a tradeoff between resolution and volume representativity. Addi-

[*]Equal contribution [1]Department of Electrical Engineering, Stanford University, Stanford, CA [2]Department of Energy Resources Engineering, Stanford University, Stanford, CA. Correspondence to: Anthony R. Kovscek <kovscek@stanford.edu>.

Proceedings of the 38^{th} International Conference on Machine Learning, PMLR 139, 2021.

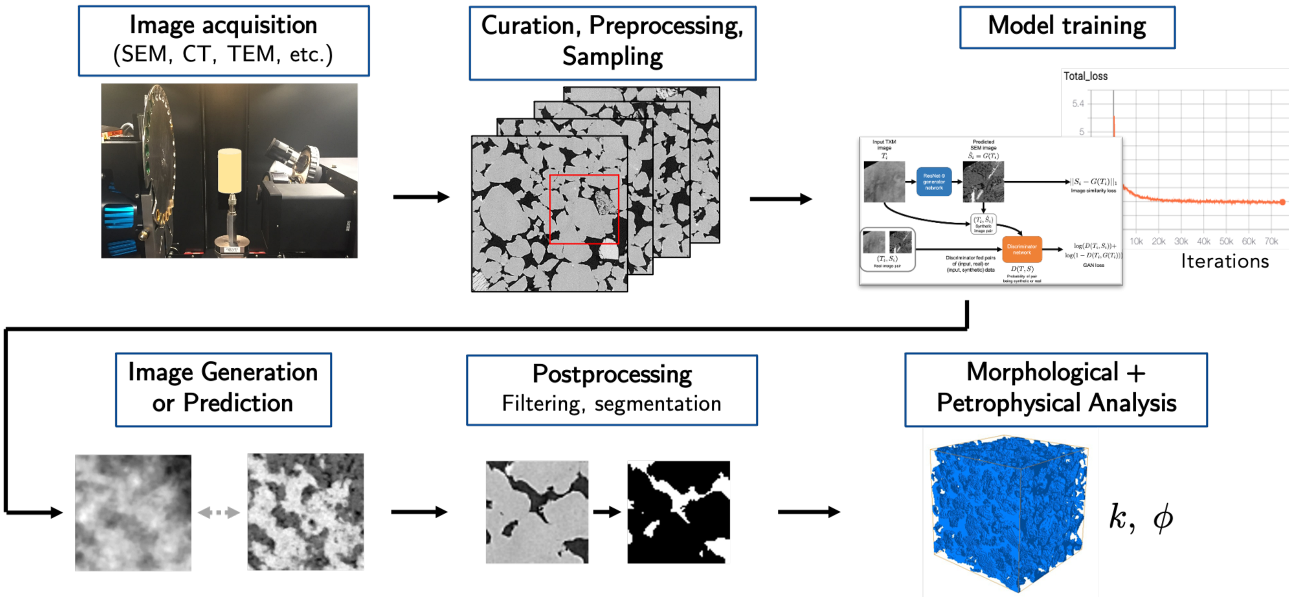

Figure 1. Machine learning image characterization workflow. Images are acquired, curated, and preprocessed into a form suitable for model training. The deep generative model is trained for applications such as image synthesis, translation, or super-resolution. The model is deployed to generate or predict images. The images are then postprocessed, often by segmentation into a simulation domain, and finally the petrophysical properties of the sample such as permeability k or porosity ϕ are analyzed.

tionally, nanoimaging is often destructive. Thus, methods with high contrast and resolution often destroy samples to acquire small image volumes (Sondergeld et al., 2010), while sample-preserving methods often have comparatively lower contrast and resolution. Translation between image domains using multimodal imaging offers the potential to predict high-resolution images suitable for segmentation and estimation of transport properties from low-resolution, non-destructive images.

2.2. Volume Translation Approach

In this application, we seek to predict destructively-acquired focused ion beam-scanning electron microscopy (FIB-SEM) images from non-destructive nano-computed tomography (nano-CT) images (Anderson et al., 2020b). Predicting FIB-SEM images from nano-CT data is a combination of image translation and single image super-resolution (SISR), both of which require synthesis of high-resolution features and low-density mineral regions. We therefore apply two generative adversarial network (GAN) models: SR-GAN (Ledig et al., 2016) and pix2pix (Isola et al., 2017). These models have shown success in similar imaging tasks and serve as suitable baselines.

The image acquisition method restricts the data to 2D paired images, so we are limited to 2D-to-2D image prediction models. To improve image volume generation with 2D-to-2D models, we use a Jacobian regularization term in the model training to encourage sparse z-gradients in the predicted FIB-SEM volume (Fig. 2). Our approach is inspired by work on robust learning (Hoffman et al., 2019) and is comparable to regularizing the model to reduce the sensitivity of network outputs to inputs.

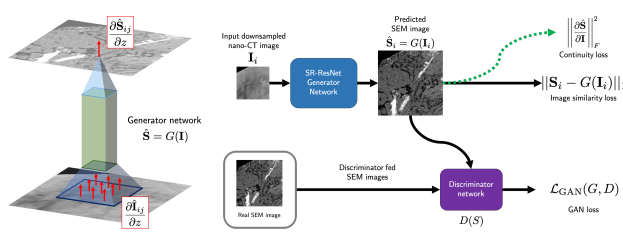

(a) (b)

Figure 2. Image prediction model. (a) Depiction of nano-CT image gradients propagating through the generator network to the output image, (b) SR-GAN model with Jacobian regularization term.

2.3. Volume Translation Results

Synthesized image volumes using baseline and regularized SR-GAN models are shown in Fig. 3. These volumes are synthesized by training 2D-to-2D image generation models, then independently passing $x - y$ plane image slices of the nano-CT volume through the generator network. In the synthesized volumes, we see that the regularized model produces more continuous image features across slices.

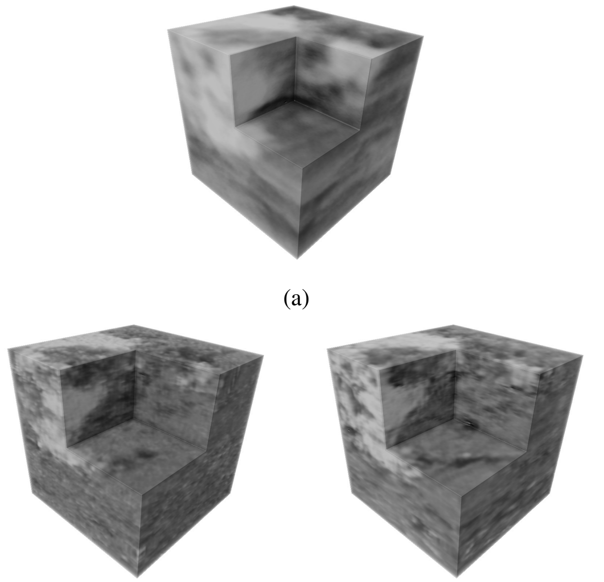

(a)

(b) (c)

Figure 3. Image volume synthesis results for SR-GAN model. (a) Input nano-CT volume, (b) Synthesized image volume without regularization (baseline model), and (c) Synthesized image with regularization. Lighter shading indicates more dense minerals.

2.4. Flow Evaluation and Visualization

Characterizing flow paths and properties such as permeability is critical for understanding the reactive transport properties of reservoir rocks. To visualize flow in the rock volume, we create a simulation domain by thresholding the lower-density regions of the translated image volume because flow is known to take place primarily in the kerogen and lower-density mineral regions.

We simulate flow in the z-direction by using a finite volume permeability solver in the PerGeos software package. Methane is introduced from the inlet at 1 MPa, with a 10^{-2} MPa pressure drop in the z-direction. The resulting pressure

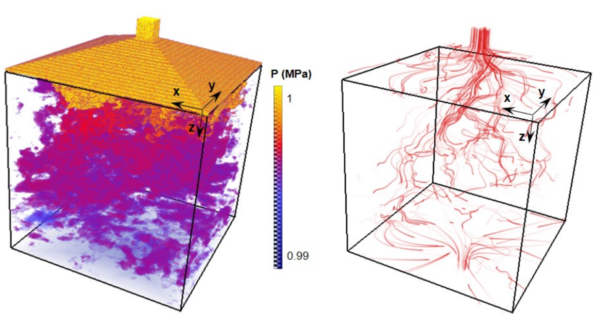

(a) (b)

Figure 4. Flow simulation results for the regularized SR-GAN model. (a) Pressure field (b) Flow streamlines.

Table 1. Comparison of permeability k, porosity ϕ, and connected porosity $\phi_{\text{connected}}$ predicted by the original and regularized SR-GAN models.

Model	k (d)	ϕ	$\phi_{\text{connected}}$
Original	2.37×10^{-5}	20.7%	18.7%
Regularized	3.01×10^{-5}	18.9%	17.4%

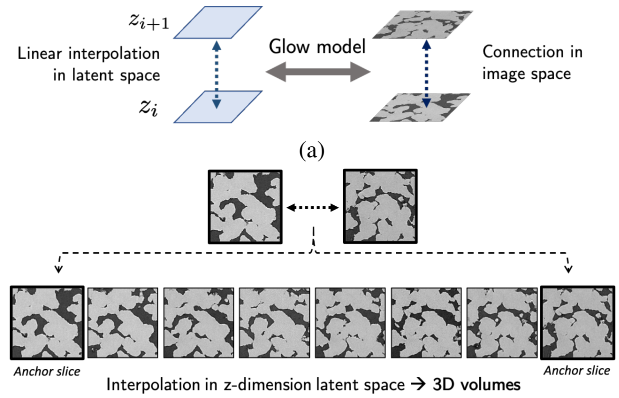

(a)

(b)

Figure 5. Volume generation algorithm. (a) Latent space interpolation. (b) Anchor slices are independently sampled, intermediate slices computed by taking an affine combination of the latent representation of the anchor slices, and the slices stacked to form an image volume.

field and flow streamlines are shown in Fig. 4a and Fig. 4b. The results for apparent permeability (measured by Darcy's law) and porosity appear in Table 1.

3. Rock Volume Generation

3.1. Volume Synthesis Approach

Deep generative models can also be a valuable tool for overcoming data scarcity in image-based characterization of reservoir rocks. In such an approach, a generative model for geological sample images is trained to sample new images of a given data volume, then petrophysical properties are estimated from these samples (Adler et al., 1990). Many generative models based on GANs or multipoint statistics have been proposed (Okabe & Blunt, 2004; Mosser et al., 2017), but these existing models either require 3D training data for 3D grayscale generation or are limited to binary image generation from 2D training data. Furthermore, synthesis of multimodal rock images remains entirely unexplored.

To overcome these obstacles, we propose a method based on generative flow models (Dinh et al., 2015; Kingma & Dhariwal, 2018). Generative flow models learn an invertible mapping $\mathbf{z} = G_\theta(\mathbf{x})$ between a datapoint $\mathbf{x}$ and latent random variable $\mathbf{z}$ with a known distribution. This allows for

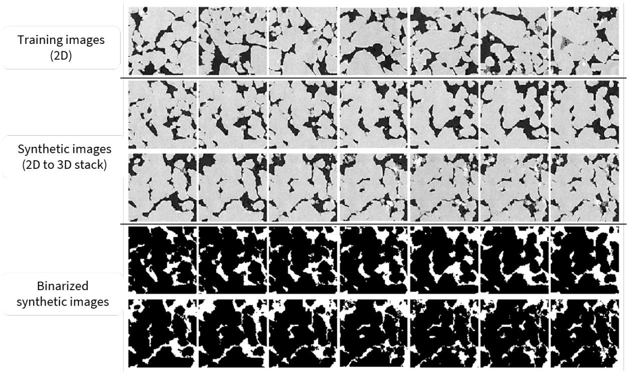

Figure 6. Bentheimer sandstone images. The synthesized images form a connected sequence of 14 images. The images are segmented into pore and grain phase to compute morphological descriptors and flow properties.

sampling new datapoints by feeding new $\mathbf{z}$ vectors into the reversed function $G^{-1}(\cdot)$. Flow models have been shown to have a latent space interpolation property where linear interpolation in latent space yields semantic interpolation in image space (Fig. 5a). We propose to use this property to generate sequences of connected porous media images by sampling latent vectors for "anchor slices" and generating the intermediate images by taking an affine combination of the anchor slice latent representations, as shown in Fig. 5b.

3.2. Image Synthesis Results

Figure 6 shows training data and synthesized images generated with our model for a Bentheimer sandstone sample. Visually, the synthetic images closely resemble the training images. The generated Bentheimer sandstone volumes also closely match the ground truth data in terms of 3D Minkowski functionals, as shown in Fig. 7. Minkowski functionals are morphological descriptors for a solid body that correlate with properties of porous media, and are therefore important to replicate in synthesized rock samples. The Glow model-based generation algorithm obtains close matches for the porosity, surface area, and Euler characteristic but differs for the mean breadth. This is likely an artifact from the image generation process and is explained in further detail in (Guan et al., 2020).

Our volume synthesis approach is also uniquely capable of multimodal image generation from 2D image data (Anderson et al., 2020a), as shown in Fig. 8. These results demonstrate the applicability of this algorithm for generation of a wide class of porous media volumes from sparse or 2D training data.

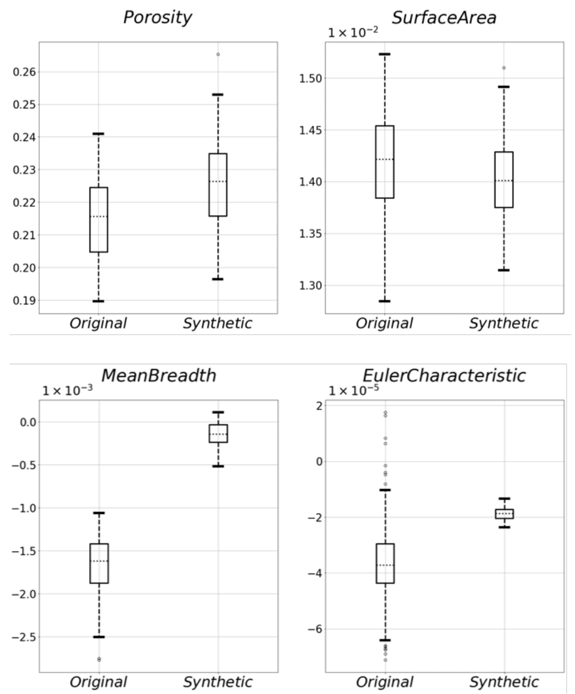

Figure 7. Minkowski functionals for synthesized Bentheimer sandstone images. The synthetic rock volumes have distributions for the porosity, surface area, and Euler characteristic similar to those found for the original images, while the mean breadth differs for the synthetic images.

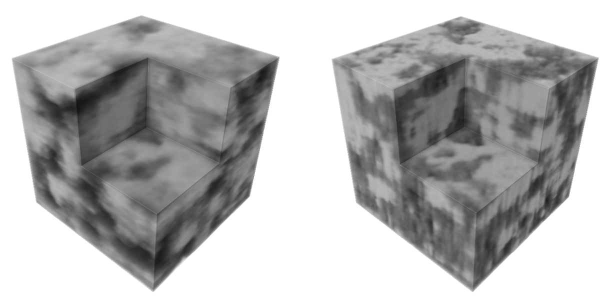

(a) (b)

Figure 8. Multimodal image generation: (a) Synthesized TXM image volume, (b) Synthesized FIB-SEM volume.

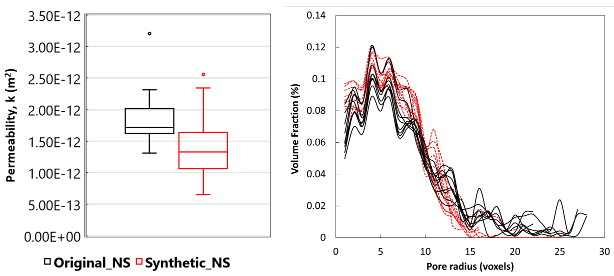

(a) (b)

Figure 9. Comparison of flow and morphological properties of Bentheimer sandstone values. (a) Distributions of apparent permeability values computed with a Navier-Stokes solver. (b) Pore size distributions for the real and synthetic Bentheimer volumes.

3.3. Evaluation of Petrophysical Properties

We also compute petrophysical properties of the predicted image volumes to evaluate the accuracy of the flow properties for the synthesized images. Figure 9a compares the single-phase permeability values obtained from a Navier-Stokes simulation and Fig. 9b compares the pore size distribution for the Bentheimer sandstone dataset. The original and synthetic volumes have a similar distribution of permeability values and pore sizes, shown respectively as the box plots and pore radius curves, showing that this approach to porous media synthesis is able to create rock sample images with realistic petrophysical properties.

4. Discussion and Conclusion

The image translation results show that the Jacobian regularization significantly improves the quality of the predicted image volume when only 2D training data is available. The cross-sections in the regularized volumes qualitatively resemble the image generation planes. We assume that at this scale, rock image features should be approximately isotropic, so the $x-z$ and $y-z$ plane slices resembling the $x-y$ plane slices show the effectiveness of the model. The apparent permeability values, while greater than what would be expected for a shale sample at the rock fabric scale, are still within the order of magnitude expected.

The image synthesis results similarly demonstrate the ability of deep generative models to create realistic image volumes. The visual similarity, permeability, and pore size distribution results show that that generated rock volumes are accurate in terms of structural and petrophysical properties. The flow model-based algorithm is also able to generalize to 3D grayscale and multimodal image generation when only 2D data is available, enabling synthesis of data from a much wider range of resolution scales, modalities, and rock samples.

Overall, this work shows the ability of deep generative models to improve characterization of reservoir rocks from limited, non-destructive, or planar image data. By enabling new characterization approaches, this work allows for better understanding of flow and reactivity in subsurface formations relevant to natural gas recovery and CO_2 and H_2 storage. In turn, we hope that this advancement helps bring us one step closer to reduced-carbon and carbon negative energy processes necessary for a sustainable future.

Software and Data

Code for this project is available at https://github.com/supri-a/TXM2SEM and https://github.com/supri-a/rockflow. Our implementation is based on the frameworks provided by Isola et al. (2017), Zhu et al. (2017), and van Amersfoort (2019).

Acknowledgements

This work was supported as part of the Center for Mechanistic Control of Water-Hydrocarbon-Rock Interactions in Unconventional and Tight Oil Formations (CMC-UF), an Energy Frontier Research Center funded by the U.S. Department of Energy (DOE), Office of Science, Basic Energy Sciences (BES), under Award # DE-SC0019165. Use of the Stanford Synchrotron Radiation Lightsource, SLAC National Accelerator Laboratory, is supported by the U.S. Department of Energy, Office of Science, Office of Basic Energy Sciences under Contract No. DE-AC02-76SF00515. Part of this work was performed at the Stanford Nano Shared Facilities (SNSF), supported by the NSF under award ECCS-2026822. We also thank Mathworks for their support of this project. Thank you to Dr. P. Creux for performing the Navier-Stokes simulations shown here. Also many thanks to Dr. C. M. Ross, M. Murugesu, and Y. Perez-Claro for helpful discussions related to this work. We thank Dassault Systèmes for providing computational resources for the LBM calculations. We thank the Stanford Center for Computational Earth & Environmental Sciences (CEES) for providing computational resources for the NS calculations.

References

Adler, P., Jacquin, C., and Quiblier, J. Flow in simulated porous media. *International Journal of Multiphase Flow*, 16(4):691 – 712, 1990. ISSN 0301-9322. doi: https://doi.org/10.1016/0301-9322(90)90025-E. URL http://www.sciencedirect.com/science/article/pii/030193229090025E.

Aljamaan, H., Ross, C. M., and Kovscek, A. R. Multiscale imaging of gas storage in shales. *SPE Journal*, 22(06):

1–760, 2017.

Anderson, T. I., Guan, K. M., Vega, B., Aryana, S. A., and Kovscek, A. R. Rockflow: Fast generation of synthetic source rock images using generative flow models. *Energies*, 13(24), 2020a. ISSN 1996-1073. doi: 10.3390/en13246571. URL https://www.mdpi.com/1996-1073/13/24/6571.

Anderson, T. I., Vega, B., and Kovscek, A. R. Multimodal imaging and machine learning to enhance microscope images of shale. *Computers and Geosciences*, 145(June): 104593, 2020b. ISSN 0098-3004. doi: 10.1016/j.cageo.2020.104593. URL https://doi.org/10.1016/j.cageo.2020.104593.

Cao, X., Yang, J., Wang, L., Xue, Z., Wang, Q., and Shen, D. Deep learning based inter-modality image registration supervised by intra-modality similarity. In *International Workshop on Machine Learning in Medical Imaging*, pp. 55–63. Springer, 2018.

Dinh, L., Krueger, D., and Bengio, Y. NICE: Non-linear independent components estimation. *3rd International Conference on Learning Representations, ICLR 2015 - Workshop Track Proceedings*, 1(2):1–13, 2015.

EIA/ARI. Eia/ari world shale gas and shale oil resource assessment. 2013. URL https://www.eia.gov/analysis/studies/worldshalegas/archive/2013/pdf/fullreport_2013.pdf.

Guan, K., Anderson, T., Creux, P., and Kovscek, A. Reconstructing porous media using generative flow networks. *Computers & Geosciences*, in review, 2020.

Hassanpouryouzband, A., Joonaki, E., Edlmann, K., and Haszeldine, R. S. Offshore geological storage of hydrogen: Is this our best option to achieve net-zero? *ACS Energy Letters*, pp. 2181–2186, May 2021. doi: 10.1021/acsenergylett.1c00845. URL https://doi.org/10.1021/acsenergylett.1c00845.

Hoffman, J., Roberts, D. A., and Yaida, S. Robust learning with jacobian regularization, 2019.

Isola, P., Zhu, J. Y., Zhou, T., and Efros, A. A. Image-to-image translation with conditional adversarial networks. *Proceedings - 30th IEEE Conference on Computer Vision and Pattern Recognition, CVPR 2017*, 2017-Janua:5967–5976, 2017. doi: 10.1109/CVPR.2017.632.

Ketcham, R. A. and Carlson, W. D. Acquisition, optimization and interpretation of x-ray computed tomographic imagery: Applications to the geosciences. *Computers and Geosciences*, 27(4):381–400, 2001. ISSN 00983004. doi: 10.1016/S0098-3004(00)00116-3.

Kingma, D. P. and Dhariwal, P. Glow: Generative flow with invertible 1×1 convolutions. *Advances in Neural Information Processing Systems*, 2018-Decem:10215–10224, 2018. ISSN 10495258.

Ledig, C., Theis, L., Huszar, F., Caballero, J., Cunningham, A., Acosta, A., Aitken, A., Tejani, A., Totz, J., Wang, Z., and Shi, W. Photo-Realistic Single Image Super-Resolution Using a Generative Adversarial Network. 2016. ISSN 0018-5043. doi: 10.1109/CVPR.2017.19.

Mosser, L., Dubrule, O., and Blunt, M. J. Reconstruction of three-dimensional porous media using generative adversarial neural networks. *Physical Review E*, 96(4), 2017. ISSN 24700053. doi: 10.1103/PhysRevE.96.043309.

Okabe, H. and Blunt, M. J. Prediction of permeability for porous media reconstructed using multiple-point statistics. *Physical Review E - Statistical Physics, Plasmas, Fluids, and Related Interdisciplinary Topics*, 70(6):10, 2004. ISSN 1063651X. doi: 10.1103/PhysRevE.70.066135.

Sondergeld, C. H., Ambrose, R. J., Rai, C. S., and Moncrieff, J. Micro-structural studies of gas shales. In *SPE unconventional gas conference*. Society of Petroleum Engineers, 2010.

Torrado-Carvajal, A., Herraiz, J. L., Alcain, E., Montemayor, A. S., Garcia-Canamaque, L., Hernandez-Tamames, J. A., Rozenholc, Y., and Malpica, N. Fast Patch-Based Pseudo-CT Synthesis from T1-Weighted MR Images for PET/MR Attenuation Correction in Brain Studies. *Journal of Nuclear Medicine*, 57(1):136–143, 2016. ISSN 0161-5505. doi: 10.2967/jnumed.115.156299.

van Amersfoort, J. Glow-PyTorch. https://github.com/y0ast/Glow-PyTorch, 2019.

Vega, B., Andrews, J. C., Liu, Y., Gelb, J., and Kovscek, A. Nanoscale visualization of gas shale pore and textural features. In *Unconventional resources technology conference*, pp. 1603–1613. Society of Exploration Geophysicists, American Association of Petroleum, 2013.

Zhu, J. Y., Park, T., Isola, P., and Efros, A. A. Unpaired Image-to-Image Translation Using Cycle-Consistent Adversarial Networks. *Proceedings of the IEEE International Conference on Computer Vision*, 2017-Octob:2242–2251, 2017. ISSN 15505499. doi: 10.1109/ICCV.2017.244.

Zoback, M. D. and Kohli, A. H. *Unconventional reservoir geomechanics*. Cambridge University Press, 2019.